Internal tides at Cross Seamount

Matthew Couldrey
4228 12th Avenue NE
Seattle, WA 98105
Tel: 206 816 9939
E-mail: mpc1g08@soton.ac.uk

Acknowledgements

The author would like to acknowledge everyone who helped in the preparation of this manuscript, both named and unnamed. Particular mention should be made of Charles Eriksen, whose guidance was indispensible, as well as the instructors and teaching assistant; Rick Keil, Danny Grunbaum, Kathy Newell, and Rika Andersen. The author would also like to thank the crew of the R.V. *Thomas G. Thompson* and entire OCN443/444 science party. Finally, the author's gratitude is extended to Naomi Hyland, whose support, inspiration and motivation extends beyond all mention.

Non-Technical Summary

The *R.V. Thomas G. Thompson* was used to study currents in the North Pacific Ocean over Cross Seamount, a large extinct submarine volcano South of Oahu, Hawai'i. The study took place from 31 December 2010 to 2 January 2011. An Acoustic Doppler Current Profiler (ADCP) was used to measure currents over the seamount. This is a device which uses acoustic waves to infer current speed and direction within specified depth ranges or 'bins'. Much like the tides observable at the sea surface, a phenomenon called an internal tide was suspected to be present over Cross Seamount. An internal tide is when the surface tide stimulates tidal motions within the water column. The water over the seamount is of particular interest because the seamount obstructs the way this internal tide flows. A mathematical model for the tide was created using the data collected by the ADCP as a basis. This model was applied both to shallow and deep layers of the water column. The model generated simulated currents in good accordance with the observed flows, although some discrepancies were present. The modelled tidal function varied with depth, indicating the propagation of an internal tide through the water column.

Abstract

The *R.V. Thomas G. Thompson* was used to survey the motions of the water column over Cross Seamount, a seamount in the North Pacific 250km South of Oahu, Hawai'i. The study took place over from 31 December 2010 to 2 January 2011. Using the ship's Acoustic Doppler Current Profiler (ADCP), currents over the seamount were sampled repeatedly. A semidiurnal tide appeared to account for a majority of the flows observed. These findings are in agreement with a previous study on tides in the area, though different dominant current directions were found. In addition to this tidal component, a diurnal (K_1) and an inertial constituent were also observed. A theoretical model for the tides observed was generated. This model, when applied at varying depths indicated the presence of a vertically propagating tide. The motions seen at depth, however, were not found to be 180° out phase with respect to the surface tide, as would be expected with an internal tide. This was concluded to be due to the presence of the seamount.

Introduction and Background

Vertical structure is a fundamentally integral aspect of oceanography. By understanding the physical characteristics of the water column, one can then go on to explain other physical, chemical and biological phenomena observed. The Hawaiian archipelago is an area which exhibits varied bathymetry, with numerous seamounts amid deep oceanic plains. In deep oceanic environments such as that seen around Hawai'i, stratification of the water column is an important physical property. Hawai'i's bathymetric features, such as seamounts, are known to have an effect on such stratified waters and stimulate internal waves (Cole et al. 2009). This research aims to better understand the internal motion of water over a seamount.

Internal waves are a phenomenon which influences other aspects of ocean science, so it is important to be able to quantify and understand them. An internal wave can be readily observed when the interface between two layers of fluid of differing density oscillates vertically, in a similar manner to a gravity wave (Garrett & Munk 1979). While internal waves may propagate along such an interface, this is not necessary for its presence; they may propagate throughout a given water column. The occurrence of such oscillations will have important effects on the biological, geological and physical environment, making them worthy of further scientific inquest.

Phytoplankton and zooplankton are affected by the movements of the water masses in which they reside, as they are broadly unable to resist large scale flows. Internal waves are an important agent in the vertical motion of plankton in and out of the photic zone (Kamykowski 1974). Since phytoplankton and zooplankton form the bases of numerous food chains, their movements are relevant to the location of organisms of higher trophic levels. This is especially important in Hawai'i, an area where fishing is a significant industry. Seamounts are known to show high biodiversity, especially with regard to economically important species such as tuna and billfish (Morato et al. 2010). A recent study found that particulate organic matter can be significantly more concentrated around seamounts than in the open ocean, due in part to the current structures around them (Vilas et. al. 2009). It would therefore be of interest to understand the dynamics of internal motions in such a location.

Cross Seamount is a large seamount located to the South of the main Hawaiian archipelago in the North Pacific, shown in Fig 1.1. The mount itself is located to the South of the main island chain. It is an important fishing site, as discussed earlier, and is worthy of greater scientific study. Seamounts in general are known to be important sites of mixing, showing orders of magnitude stronger mixing compared with off seamount open ocean locations (Luek, R.G. 1997). There already exists some knowledge of the nature of internal tides over Cross (Noble & Mullineaux 1989) and about the seamount itself, but no comparison of internal waves on and around the seamount has been done. Noble and Mullineaux (1989) found tidal currents over Cross Seamount to be 2-3 times stronger than those observed in the typical open Pacific, but it was unclear whether the seamount was responsible generation of this tide.

In addition to observing the motions of the water column over the seamount, this study also aims to generate a model to enumerate an internal tide beyond observation. This model will use the data collected as a basis to 'fill in the blanks' elsewhere. Comparisons between the modelled and observed data may then be drawn.

This study provides scope for further research down numerous avenues of scientific inquest. Similar future studies on other seamounts could stem from this research in the interest of comparing the effects of seamounts on internal tides. There is opportunity for the study's use in plankton dynamics over the seamount; for example, can the movements of plankton over the seamount be correlated with the internal tide over Cross? There is also use for this research in conjunction with geological surveys of the bathymetry of Cross seamount's summit; is there any relationship between bedforms or sediment transport observed and internal tides?

Methods

An ADCP current survey was carried out over Cross Seamount using the shipboard ADCP of the *R.V. Thomas G. Thompson* over 31December 2010 to 2 January 2011. The ADCP used was RD Instruments' Ocean Surveyor, operating at a frequency of 75kHz.

Figure 2.1 shows the transect lines of the ADCP survey used to sample the water column over Cross Seamount. This consisted of three diametric transects over the summit of the seamount, each 6

nm long with shorter 3nm paths connecting these transects, taking approximately four hours to complete. Each transect began and ended at waypoint 6. The path was followed in the reverse order to which the waypoints are numbered (i.e. begin at 6, proceed to 5, then 4 and so on to 1 then back to 6 to begin a new set of transects). This path was sampled 6 times over the study as consistently as possible.

The data collected from the ADCP was processed using Matlab (Version 7.0.1). The following equation served as a basis for which current could be calculated;

$$u_t = b\sin(\sigma_1 t) + c\cos(\sigma_1 t) + d\sin(\sigma_2 t) + e\cos(\sigma_2 t) + f\sin(\sigma_3 t) + g\cos(\sigma_3 t) + n$$

Current, *u*, at a given time, *t*, can be calculated using this model, assuming that constants *b* through *e* are known. Current from non-tidal origin is represented by *n*. It is assumed that *n* will chiefly consist of noise, and will be small enough to be negligible. The accuracy of this assumption will be assessed later. The frequencies of tidal modes are represented by σ, where σ_1 is the frequency of the Principal Semidiurnal Lunar tide (M_2 tide), σ_2 is that of the Lunar Diurnal (K_1 tide) and σ_3 is that of inertial current, I. This last frequency is a contributor to periodic current variations, but is due to the planet's rotation, rather than the sun or moon. For the latitude concerning this study (18.7167°N), the inertial frequency (the inverse of the Coriolis parameter) was taken to be 37.396 hours. In this study, these frequencies are computed in radians and are thus;

$$\sigma_1 = \frac{2\pi}{12.421\ hrs} \qquad \sigma_2 = \frac{2\pi}{25.819\ hrs} \qquad \sigma_3 = \frac{2\pi}{37.396\ hrs}$$

The remaining terms to be evaluated are *b* through g, which were calculated based on observed currents at Cross Seamount. Each pair of constants (*b-c*, *d-e* and *f-g*) corresponds to each of the three tidal constituents and is unique to each situation. These constants determine the relative effect that each tidal component will have on a given situation. Matlab was used to compute these values. The details of this procedure, such as the M-files used, are available upon request.

The phase difference of tidal motions was then computed. This is a way of comparing how the tide at depth 'lags' behind the tide moving at the surface. If there is a deep layer moving 180° out of phase with the surface tide, then the motions of the deep layer are attributed to the presence of an internal tide. This was done by computing the phase difference, θ, for each tidal mode separately.

$$\theta_{M2} = tan^{-1}\left(\frac{c}{b}\right) \qquad \theta_{K1} = tan^{-1}\left(\frac{d}{e}\right) \qquad \theta_{I} = tan^{-1}\left(\frac{g}{f}\right)$$

These theta values were plotted against the depth to which they corresponded. This allows for comparison of tidal phase with depth. This is done to show whether the surface currents are leading those at depth or vice versa.

Tidal ellipses were then constructed for each tidal component. These are plots of eastward against northward modelled currents. Three sets of ellipses were generated; one for each of the three tidal components. These plots allow for comparison of the different tidal components with depth, illustrating whether an internal tide is propagating vertically.

Results

Tidal Models

Tidal models for current over Cross Seamount were generated; Figures 3.1 to 3.4. Since the tides appeared to vary with depth, four depth ranges were chosen for which different tidal models would be generated. Optimum resolution of depth variance of tidal flows was found when currents were averaged into four different depth bins; 30 to 110m, 110 to 190m, 190 to 270m and 270 to 334m. Each of these depth bins were of equal size, with the exception of the last. The deepest bin had to be slightly smaller than the other bins as a result of the way the averaging process coped with the fact that the summit of the seamount obscured data beneath 334m.

Each of Figures 3.1 to 3.4 shows four plots over the course of the sampling period. Two of the plots (the red and blue) show observed anomalous current as collected by the ADCP (divided into eastward and northward components respectively). Anomalous current is the flow observed at a given time with the mean current subtracted from it. This allows for observation of periodically time-variant currents, which are the tides, with background flows removed (background flows being currents resulting from to non-tidal factors like wind, geostrophy etc.). The smoother curves (the pink and green) show modelled anomalous current (again, eastward and northward respectively) based on the observed currents in the corresponding depth band. These are ostensibly the same currents as those observed, but with missing time series filled in, calculated mathematically. Assuming the simulation

perfectly modelled the observed current (which would ideally be noise free), the curves would intersect each of the observed data points and provide perfectly accurate modelled current in the time series' gaps. The accuracy of the data and models, however, will be assessed later.

Tidal Ellipses

The tidal ellipses are shown in Figures 3.5 to 3.7. These plots show a breakdown of current by tidal component. They are plots of modelled eastward against modelled northward current according to only one tidal component at a time. Since each of the tidal components is cyclic, they plot elliptical patterns. The ellipticity is due to the fact that each of the tidal components are affected by the aforementioned constant pairs, *b-c*, *d-e* and *f-g*. These constants are in turn affected by whatever may affect tides in a given situation, such as bathymetry, coastal geomorphology, etc. A difference in ellipticity with depth shows that some such factor is affecting tides vertically.

Phase/Depth Plots

Figure 3.8 shows plots of the relative phases of tides with depth. They illustrate the differences in the relative timing of each tidal component with depth. If the whole water column was affected by the tides evenly then there would be no phase difference with depth and the plots would show straight profiles. A phase difference with depth indicates relative internal motion of the water column in the form of an internal tide. A phase difference of 180° between a surface and a deep layer would indicate the two layers moving exactly out of phase. This would mean that if tidal currents in the surface were flowing in one direction at a given time, the direction flow at depth would directly oppose that of the surface.

Discussion

Tidal Models

The models appear to show tidal variation corresponding quite well to the currents observed. The fit of all of the models, however, is not perfect. This is evident from the fact that the models' values do not exactly intersect the observed values. This is likely due to two broad areas of error. The first would be in the fact that the model is based on data which may not show tidal signal with perfect

accuracy. This is almost certainly a reason for the incongruence of modelled and observed data, since data collected by an ADCP are prone to at least some noise. Additionally, there is the inaccuracy of the mean current (from which the plotted observed data were subtracted). Another notable inaccuracy would be due to the incomplete time series collected. The time series shown only use data collected within 1 km of the central waypoint of the survey plan, since this was where the most data (and thus where the best tidal signal) were collected. Since the sampling scheme did not allow for a complete time series at a single point to be collected, there is large inaccuracy in the dataless time periods.

The second area or error corresponds to the assumptions of the model itself. It is assumed that only three tidal components will have a significant influence on tidal flows at this location; the M_2, K_1 and inertial effects due to the Earth's rotation. The others were assumed to be negligible, in the interests of simplifying the models. In reality, all tidal components affect all tides, although most have a very minor effect on observed currents. In a similar study on another Hawaiian seamount (Great Meteor), the quarter-diurnal (M_4) constituent is also accounted for and seen to have some influence at depth (Gerkema and van Haren 2007). This harmonic was omitted for this study, since its frequency (and thus effect) was taken to be too small to be observed, given the incomplete time series. It could be, however that this constituent could have yielded a greater accuracy if included. In the future, therefore, one improvement that could be made to this study could be to include the M_4, and possibly other frequency.

Despite the residual (the discrepancy between modelled and observed values), the models do appear to show a strong tidal signal which varies with depth. The most obvious frequency seen in the plots is the semidiurnal. This is therefore the constituent which has the greatest effect on tidal current on the seamount. This is in concordance with another tidal analysis of this seamount (Noble and Mullineaux, 1989) and another Hawaiian seamount (Gerkema and van Haren 2007). Such agreement indicates the validity of both observed data and the models generated. It should be noted that the relative importance of each tidal component cannot be quantified with the data collected by this study, which is something other studies have included. This presents itself as an opportunity for improvement of this study or for future research. Furthermore, Figures 3.1 to 3.4 also show a clear

variance in the tides with depth. While this is not yet quantified, it does indicate that internal motions are present, which may be the result of an internal tide.

Tidal Ellipses

The tidal ellipses, Figures 3.5 to 3.7 show notable changes in the tides with depth, for all three tidal components. The ellipses for the semidiurnal tide (Fig 3.5) show that the two shallower depth bins are quite different to the deeper two. The deepest depth bin's ellipse shows very close alignment to the East/West axis, which is what was predicted by Noble and Mullineaux (1989) in their tidal analysis of Cross Seamount. This lends credence to the data from both studies. For this frequency, particularly, the lower half of the water column appears to be moving quite differently to the top half. This change with depth is what would be expected in the presence of an internal tide, so the presence of such a tide is indicated by this plot.

The ellipses for the diurnal tides, Fig 3.6 indicate a similar depth trend to those of the semidiurnal frequency. The orientation of the ellipses for the shallowest two bins are very closely aligned, indicating again that the surface half of the water column is moving as one as a result of this frequency. The deeper two ellipses, however, do not seem as aligned as the surface pair, and also do not show the same degree of change in orientation seen by the semidiurnal frequency. This indicates that the internal tide due to this frequency is somehow obstructed. It is also interesting to note that the effect of this frequency appears greatest with depth and is quite minimal in shallow water, judging by the relative sizes of the ellipses. This is what might be expected for internal motions.

The ellipses for the inertial component of the tides, Fig 3.7 show a near circular pattern for the deepest bins, which is characteristic of an internal tide at depth. Interestingly, the change in orientation of the major axis appears to occur between the first and second depth bins, rather than between the second and third bins as was seen with the other frequencies. This indicates that for this frequency, the difference in moving layers of the internal tide is shallower than for the other frequencies.

Phase/Depth Plots

Fig 3.8 shows the changes in phase of the different tidal components with depth. This shows which layer is dragging the other. Since the semidiurnal tide is the strongest of the three components,

the phase difference for this frequency will have the greatest affect on the internal tide. The sudden change in phase and sign between the second and third bins suggests that the surface tide is dragging the deep layer, resulting in an internal tide.

The other two frequencies' plots show a less coherent phase difference with depth, indicating that the different layers are not moving perfectly out of phase. This is also seen for the semidiurnal frequency, but to a lesser extent than the other two. This lack of 180° phase difference could be due to a number of factors, but is attributed to the presence of Cross Seamount and its interference with the internal tide.

Conclusions

An internal tide signal was seen at Cross Seamount in the data collected and in the model which was then calculated. The model generated is concluded to be of acceptable accuracy, though it does have scope for further improvement with the inclusion of other tidal frequencies. The strongest tidal component appeared to be the M_2 tide, which is in agreement with other findings in literature. There was seen to be interference in the internal motion of the water column over Cross Seamount's summit which was seen in a lack of a 180° phase difference between surface and deep layers. This is concluded to be due to the presence of the seamount disrupting the horizontal and vertical propagation of internal tides.

Figures

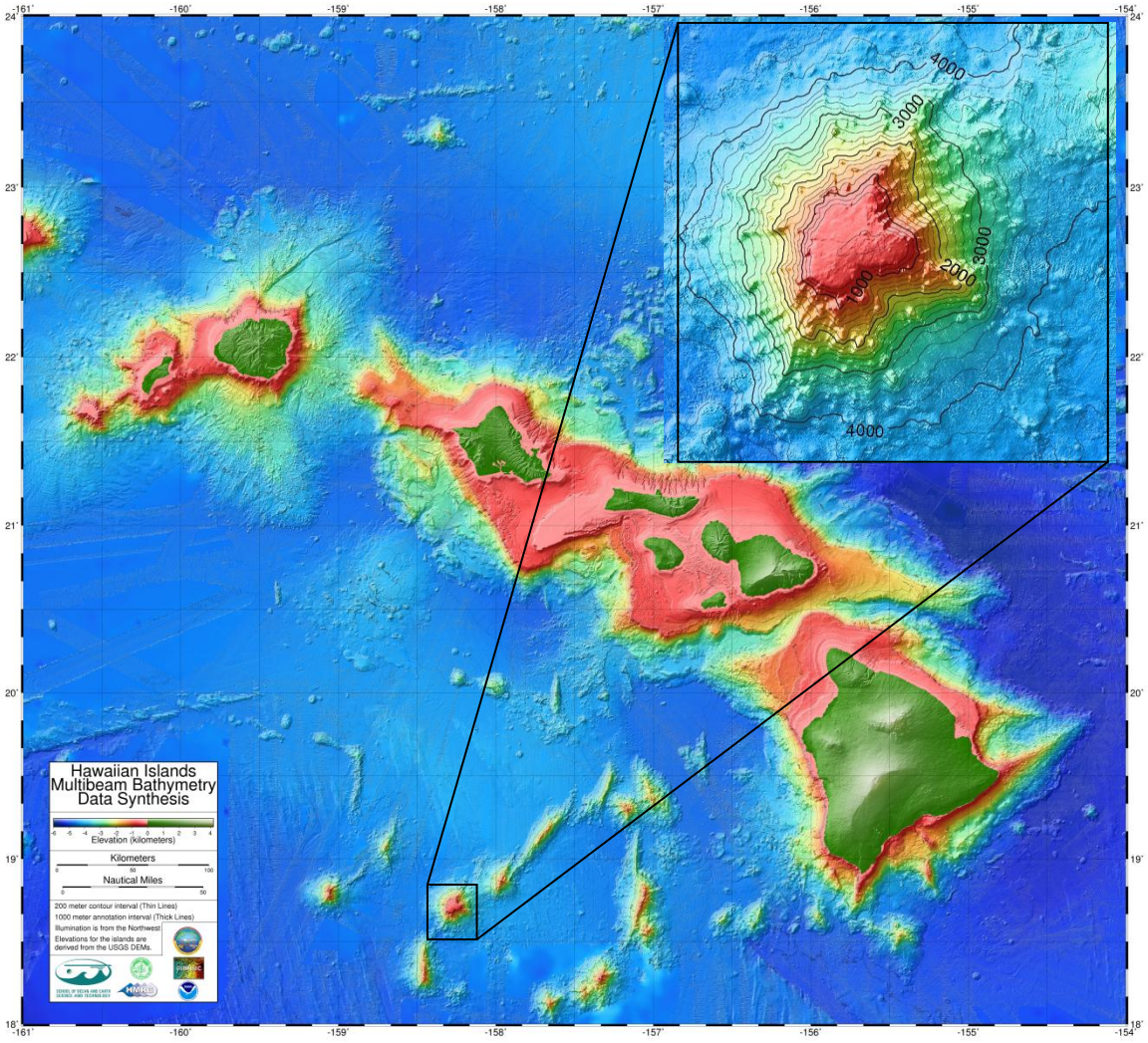

Fig 1.1 High Resolution Multibeam Bathymetry of the Hawaiian Archipelago with zoomed detail on Cross Seamount (top right) from the Hawaii Mapping Research Group, School of Ocean and Earth Science and Technology, University of Hawai'i (available http://www.soest.hawaii.edu/HMRG/multibeam/images/mhis_mb_v15a.jpg?file=mhis_mb_v9r.jpg)

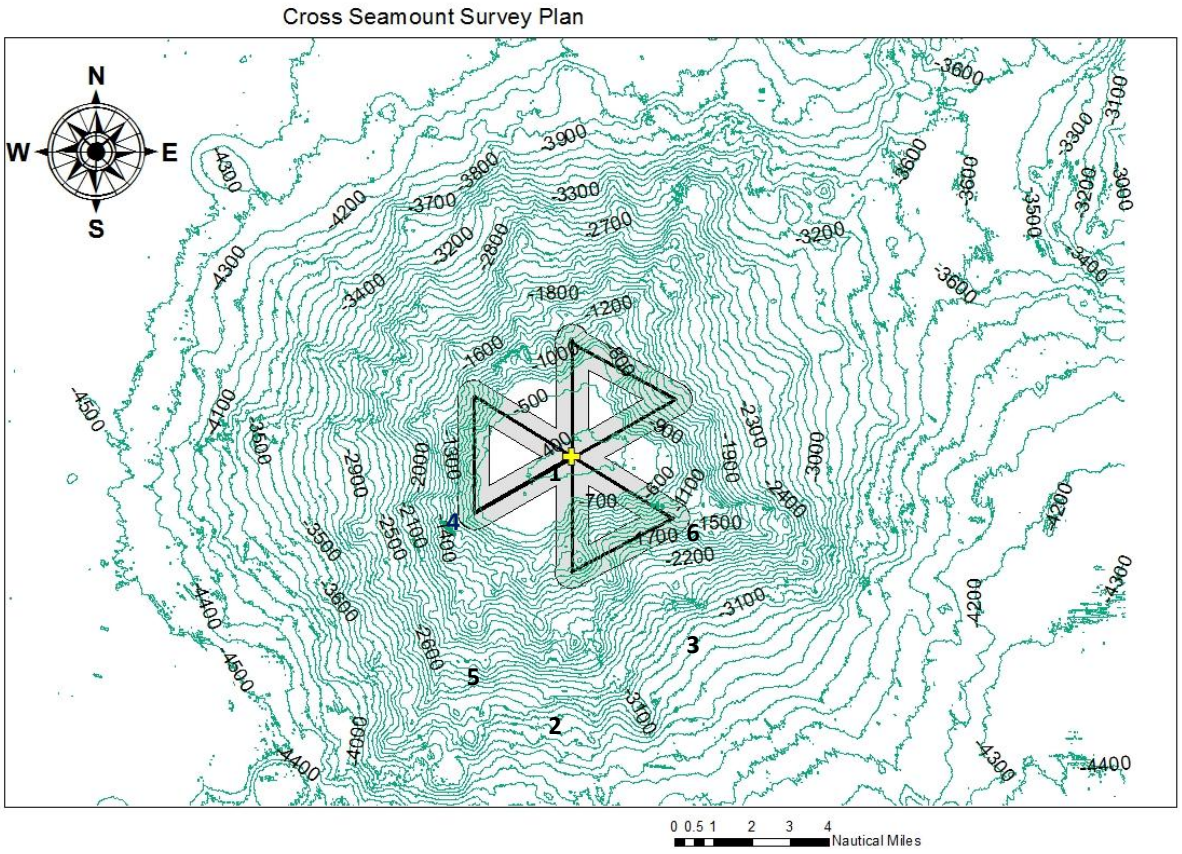

Fig 2.1 Bathymetry of Cross Seamount with the survey plan superposed. Isobaths are in metres, the corners of survey, or waypoints, are numbered 1-6. The yellow '+' shows the centre waypoint, C.

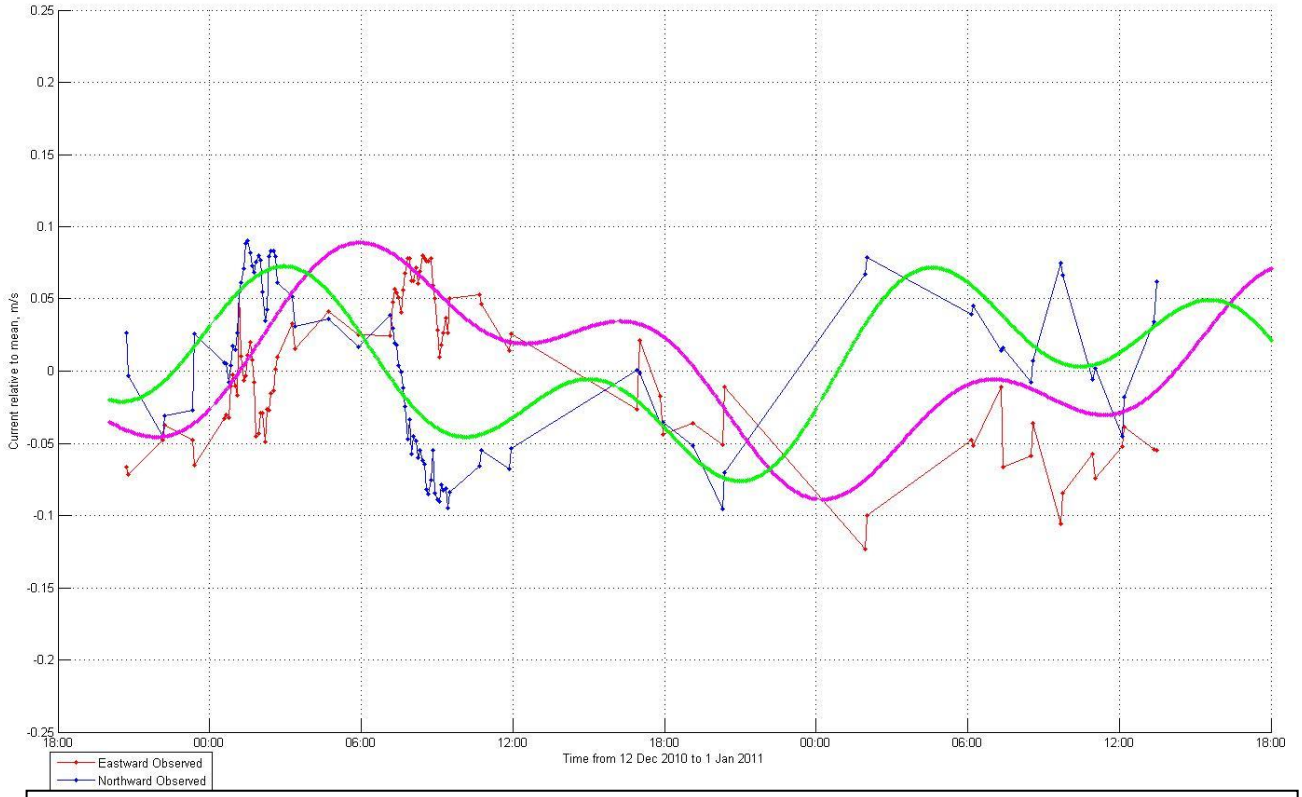

Figure 3.1 Anomalous current time series showing both observed and modelled eastward and northward current for the depth range 30 to 110m

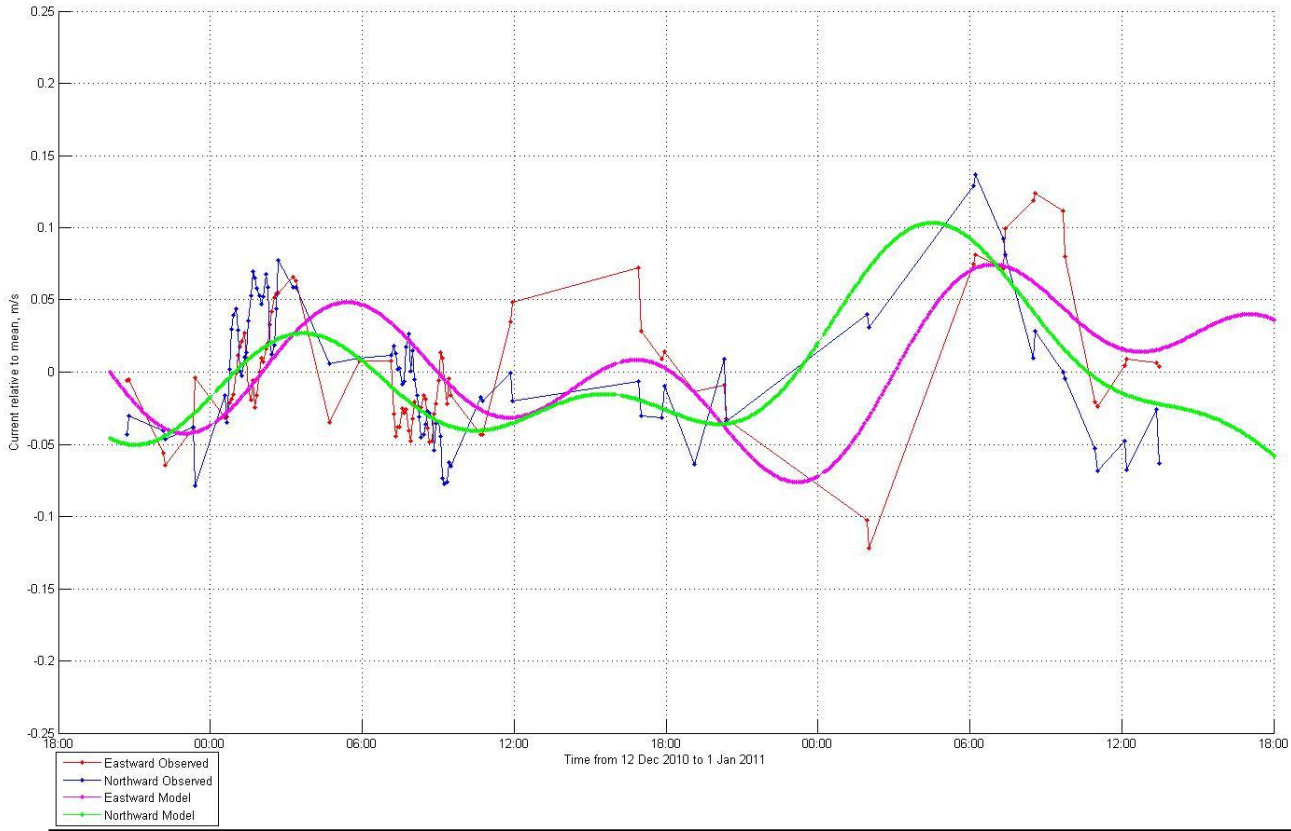

Figure 3.2 Anomalous current time series showing both observed and modelled eastward and northward current for the depth range 110 to 190m

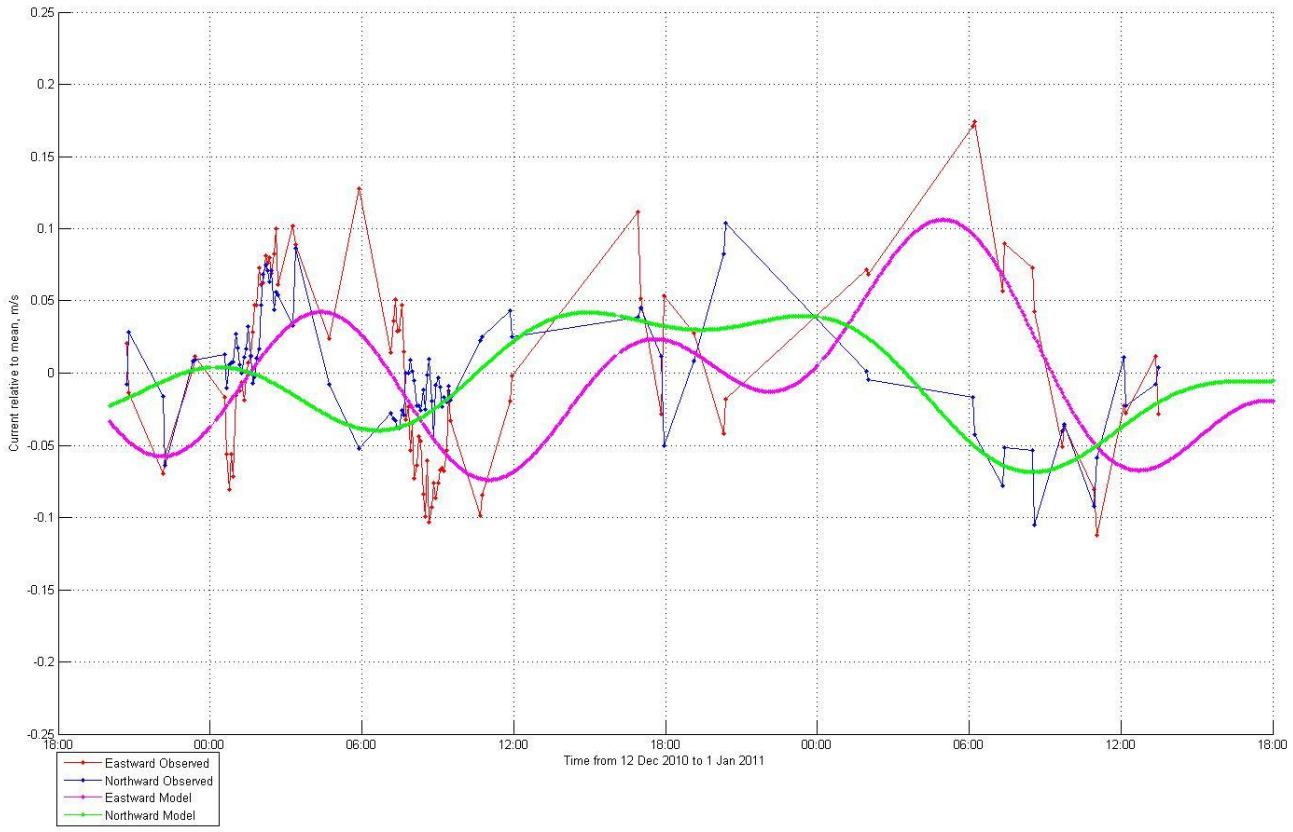

Figure 3.3 Anomalous current time series showing both observed and modelled eastward and northward current for the depth range 190 to 270m

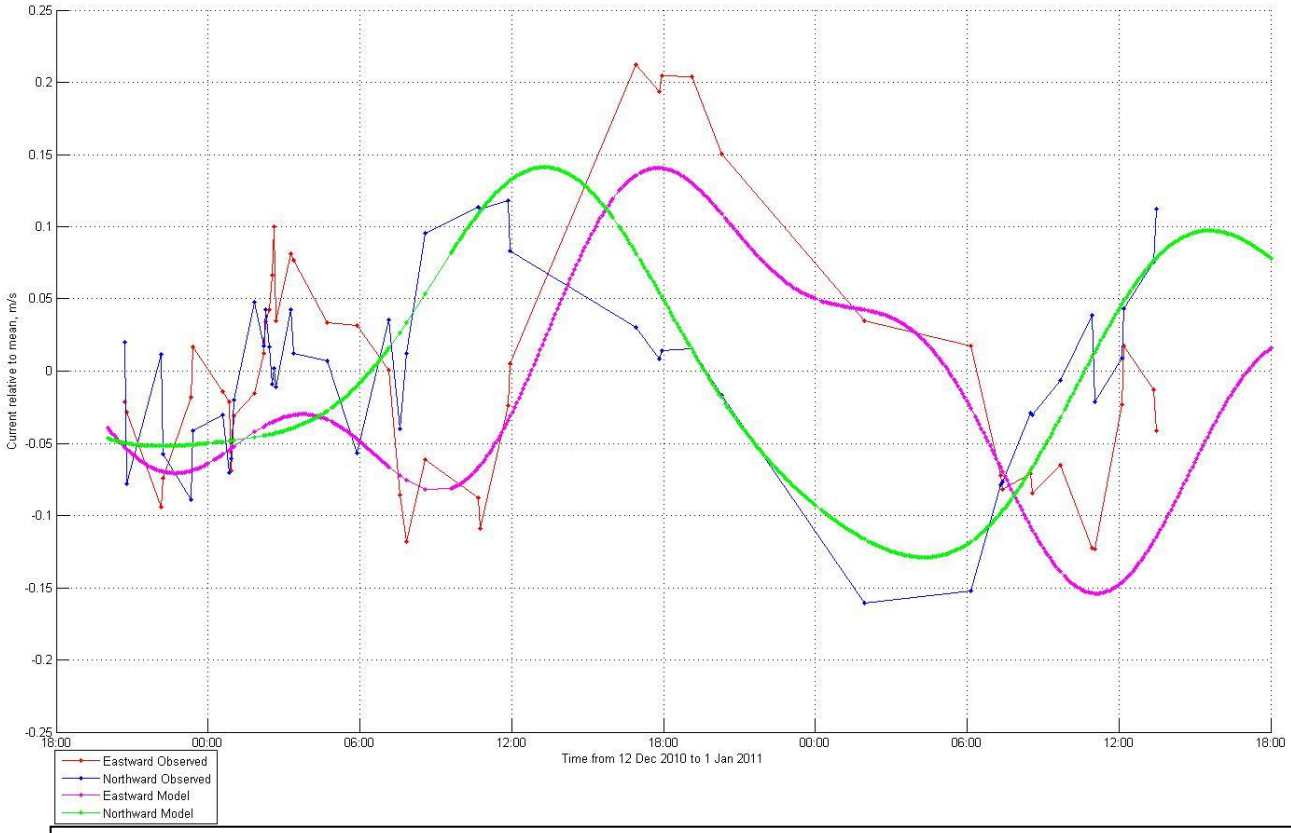

Figure 3.4 Anomalous current time series showing both observed and modelled eastward and northward current for the depth range 270 to 334m

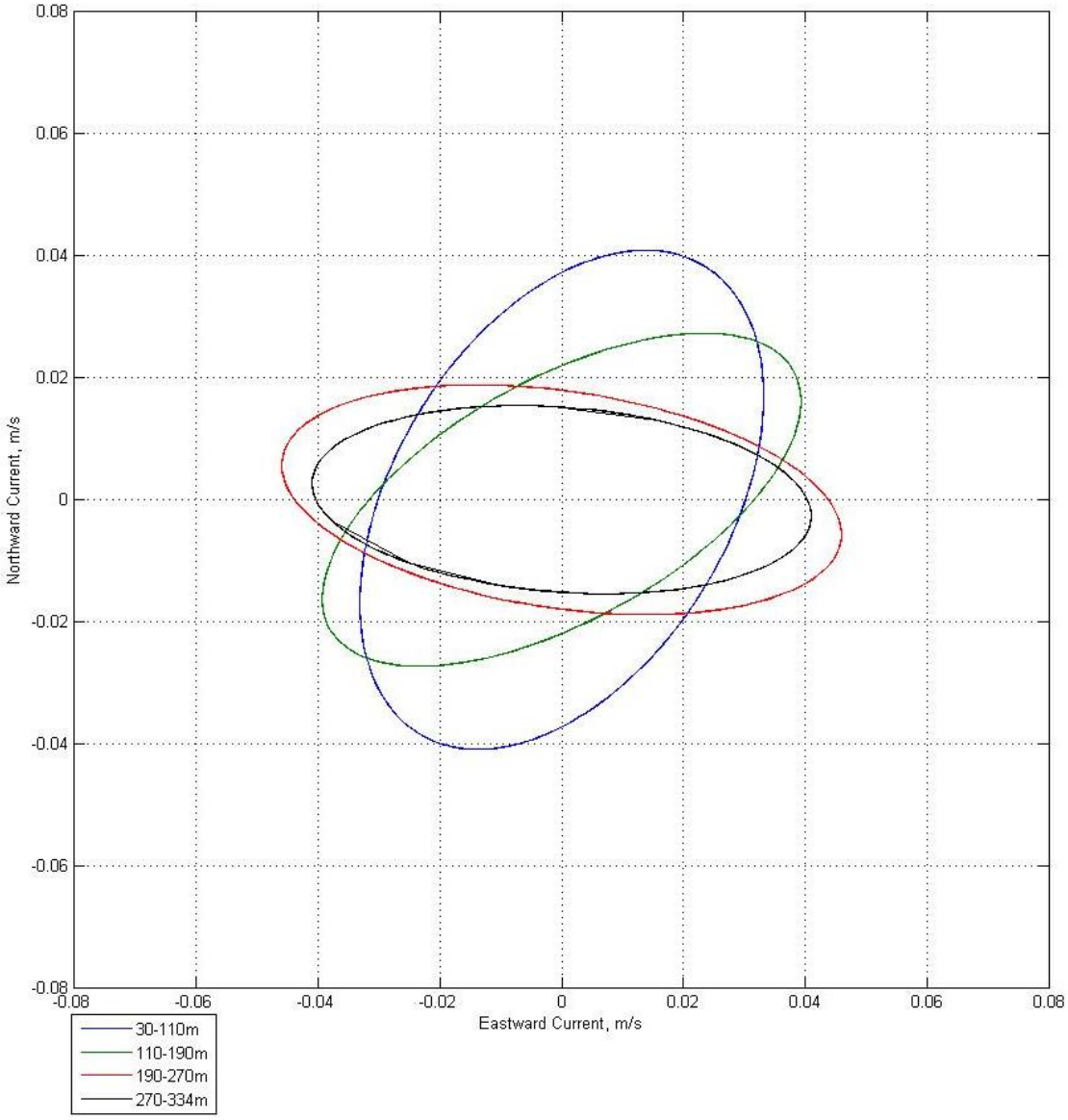

Figure 3.5 Tidal ellipses showing ellipses for each of the four depth bins for the semidiurnal frequency

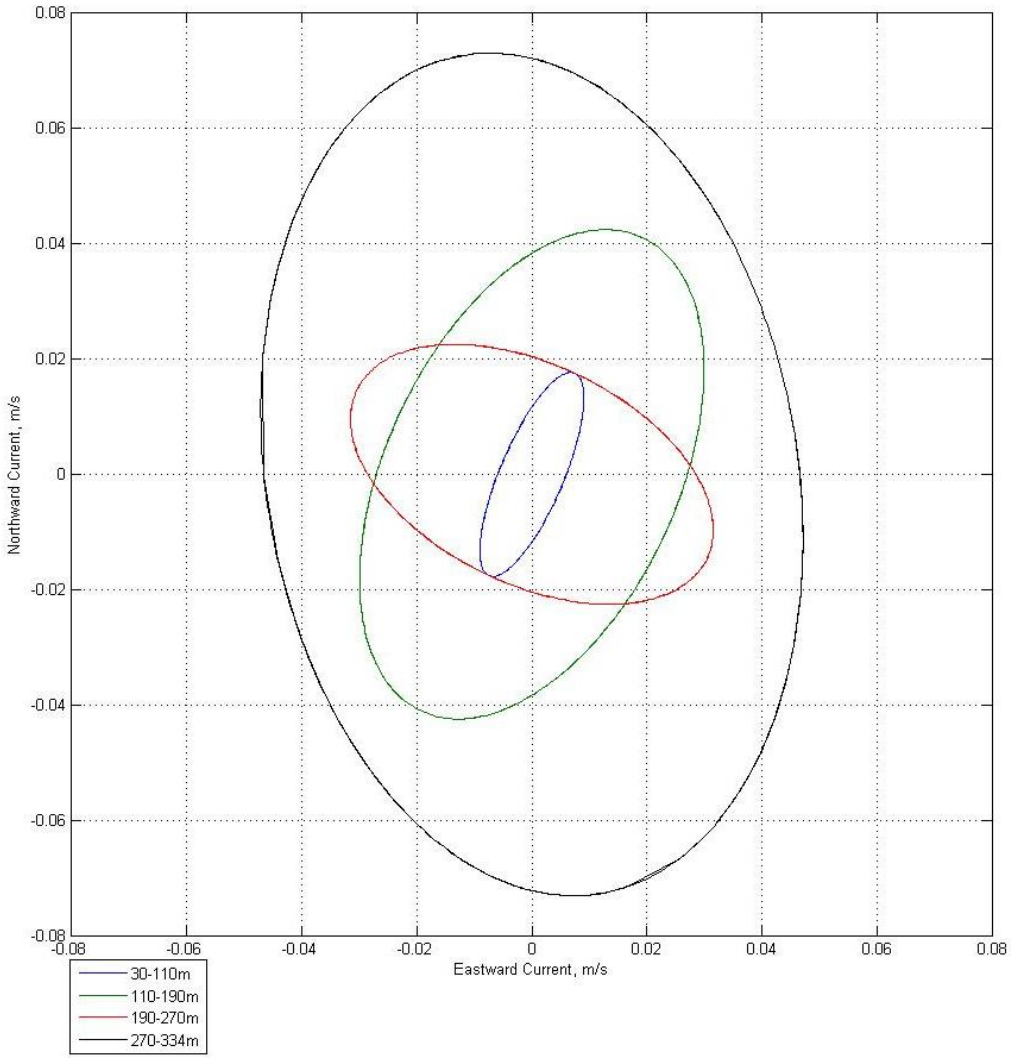

Figure 3.6 Tidal ellipses showing ellipses for each of the four depth bins for the diurnal frequency

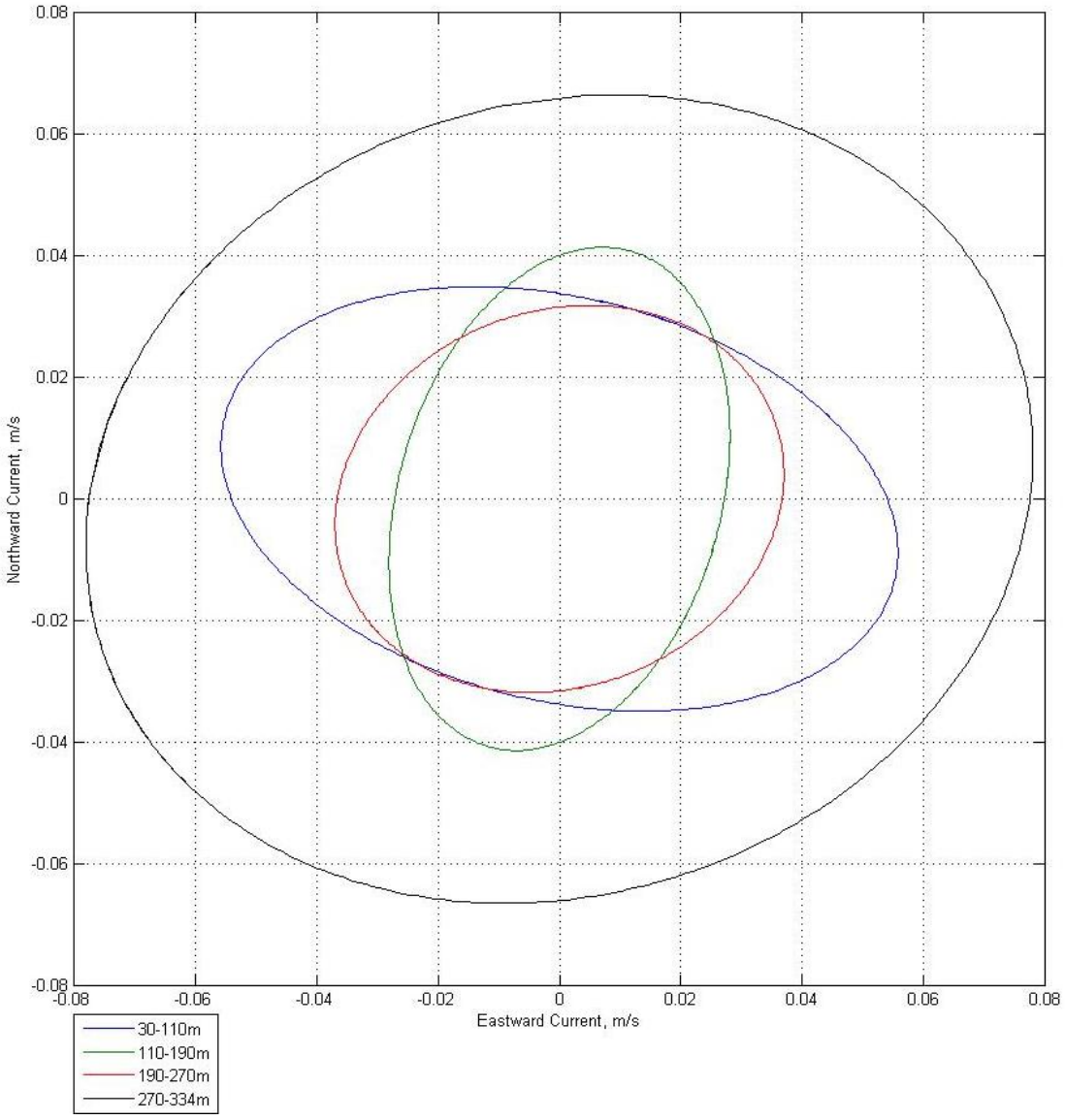

Figure 3.7 Tidal ellipses showing ellipses for each of the four depth bins for the inertial frequency

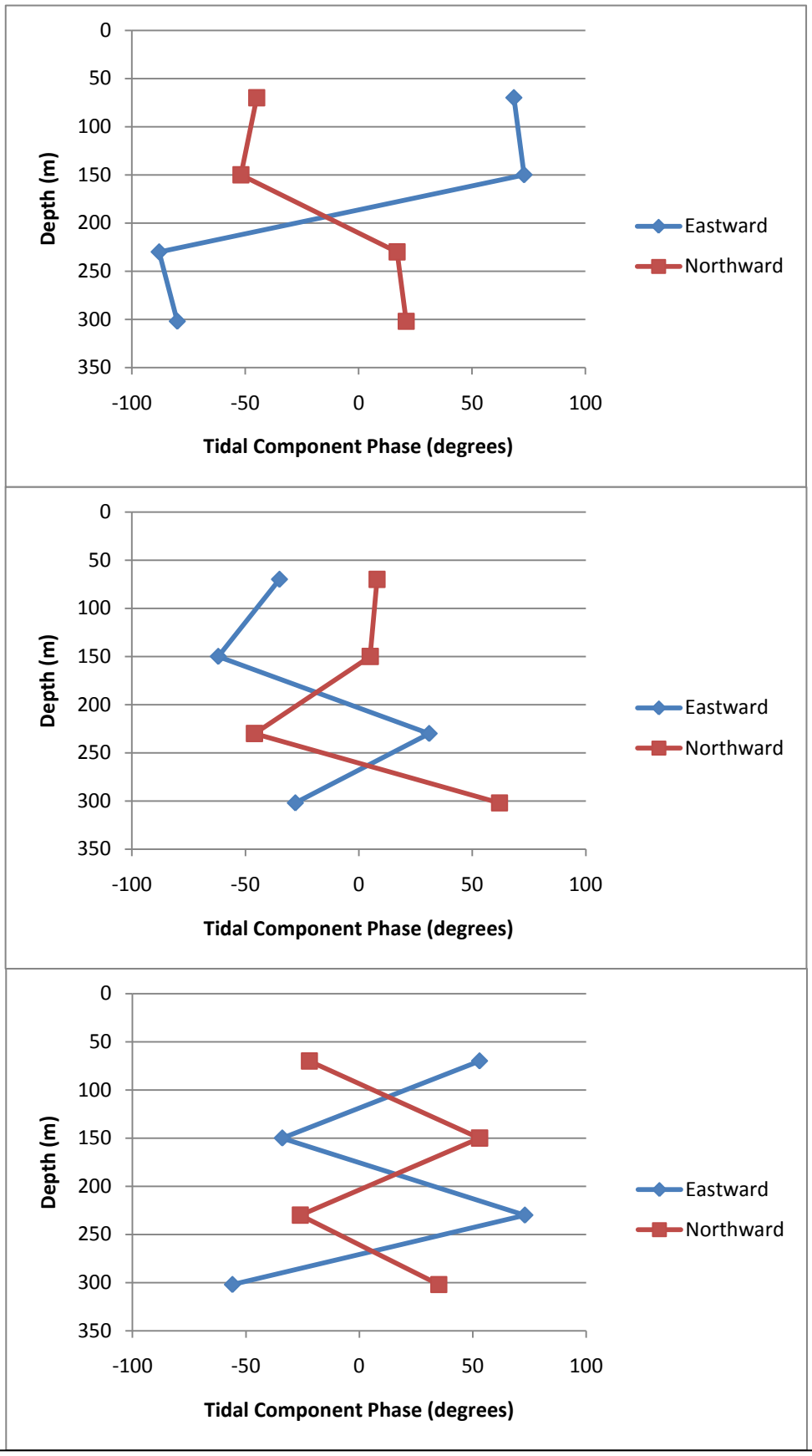

Figure 3.8 Tidal phase/depth plots showing the different phases of tides with depth for the semidiurnal, diurnal and inertial components (from top to bottom)

References

Cacchione, D.A., Schwab, W.C., Noble, M. & Tate, G. 1988. Internal tides and sediment movement on Horizon Guyot, Mid-Pacific Mountains. Geo-Marine Letters, 8: 11-17

Cole, S.T., Rudnick, D.L. & Hodges, B.A. 2009. Observations of Tidal Internal Wave Beams at Kauai Channel, Hawaii. J. Phys. Oceanogr. 39: 421-436

Flatté, S.M., Dashen, R., Munk, W.H., Watson, K. & Zachariasen, F. 1979. Sound Transmission through a Fluctuating Ocean. Cambridge University Press.

Garrett, C. & Munk, W. 1979. Internal Waves In The Ocean. Ann. Rev. Fluid Mech. 11:339-69

Gerkema, T. & van Haren, H. 2007. Internal tides and energy fluxes of Great Meteor Seamount. Ocean Science, 3, 441-449.

Horn, W. 1971. Die zeitliche Veranderlichkeit der Temperatur der ozeanischen Deckschicht in Gebiet der Grossen Meterobank [The temporal variation of the temperature of the oceanic surface layer in the Large Meterobank zone]. Meteor Forschungsergebneisse. 9, 47-57

Kamykowski, D. 1974. Possible interactions between phytoplankton and semidiurnal internal tides. J. Geophys. Res. 80:1163-1167

Karl, H.A., Cacchione, D.A. & Carlson, P.R. Internal-wave currents as a mechanism to account for large sand waves in Navarinsky Canyon head, Bearing Sea. J. Sed. Pet. 56, 5:706-714

Kundu, P.K. & Beardsley, R.C. 1991. Evidence of a Critical Richardson Number in moored measurements during the upwelling season off Northern California. J. Geophys. Res. 96: 4855-68.

Luek, R. G. & Mudge, T.D. 1997. Topographically Induced Mixing Around a Shallow Seamount. Science. 276, 5320: 1831-1833

Morato, T., Hoyle, S. D., Allain, V. & Nicol, S. J. 2010. Seamounts are hotspots of pelagic biodiversity in the open ocean. Proc. Natl. Acad. Sci. USA. 107, 21: 9707-9711

Munroe, J.R. & Lamb, K.G. 2005. Topographic amplitude dependence of internal wave generation by tidal forcing over idealized three-dimensional topography. J. Geophys. Res. Vol: 100. C02001, doi:10.1029/2004JC002537.

Noble, M. & Mullineaux, L.S. 1989. Internal tidal currents over the summit of Cross Seamount. Deep-Sea Research, 36, 12: 1791-1802

Richardson, L.F. 1920. The supply of energy from and to atmospheric eddies. Proceedings of the Royal Society of London. Series A, Containing Papers of a Mathematical and Physical Character. 97, 686: 354-73.

Venugopal, V. & Smith, G.H. 2007. Wave climate investigation for an array of wave power devices. Proceedings of the 7th European Wave and Tidal Energy Conference.

Vilas, J.C., Arístegui, J., Kiriakoulakis, K., Wolff, G.A., Espino, M., Polo, I., Montero, M.F. & Mendonça, A. 2009. Seamounts and organic matter- Is there an effect? The case of Sedlo and Seine Seamounts: Part 1. Distributions of dissolved and particulate organic matter. J. Deep-Sea Res. II, 56: 2618-30